



---

## THICKNESS DEPENDENT PHYSICAL PROPERTIES OF ELECTRON BEAM EVAPORATED COPPER OXIDE THIN FILMS

**V. Sravanthi, T. Srikanth, R. Subba Reddy and A. Sivasankar Reddy\***

Department of Physics, Vikrama Simhapuri University Postgraduate Centre, Kavali -524201, Andhra Pradesh, India

**P. Sreedhara Reddy**

Department of Physics, Sri Venkateswara University, Tirupati- 517502, Andhra Pradesh, India

**Ch. Seshendra Reddy**

Department of Materials Science and Engineering, Harbin Institute of Technology, University Town, Shenzhen, 518055, China

*\*Corresponding author: A. Sivasankar Reddy*

### ABSTRACT

*Cuprous oxide ( $Cu_2O$ ) thin films were deposited on glass substrates by electron beam evaporation at different film thicknesses. The films have excess oxygen at the film thickness of 133nm and the films deposited at thickness of 192nm were nearly stoichiometric. As increasing the films thickness, the peak intensity and the polycrystalline nature increased. The calculated stress values are -0.57, -0.34 and -0.83GPa for 133, 192 and 257nm. The surface roughness of the films decreased with increasing the film thickness upto 192nm, and it increased at higher film thickness. The poor optical transmittance was observed at low and very high thickness films.*

**KEYWORDS:** Cuprous Oxide; Electron Beam Evaporation; Thickness; Thin Films

## 1. INTRODUCTION

Cuprous oxide ( $\text{Cu}_2\text{O}$ ) has wide range of applications including solar cells, sensors, photocatalysts, lithium ion batteries, transparent displays [1]-[4], because of its unique properties such as, high absorption coefficient in the visible light region, nontoxicity, abundance, band gap of  $\sim 2.1\text{eV}$ , and low fabrication cost [5]-[7]. Various thin film deposition techniques such as, sol-gel [8], electrochemical deposition [9], thermal oxidation [10], sputtering [11] and electron beam evaporation [12] have been used to prepare the  $\text{Cu}_2\text{O}$  films. Among these deposition techniques, electron beam evaporation (EBE) is a versatile technique due to its unique properties. The properties of the electron beam evaporated films are mainly depends on the deposition parameters such as substrate temperature, target to source distance, accelerating voltage, thickness, etc. In the present work,  $\text{Cu}_2\text{O}$  films were deposited on the glass substrates at different films thickness and studied the compositional, structural, surface morphology, electrical and optical properties of the as deposited films.

## 2. EXPERIMENTAL

The  $\text{Cu}_2\text{O}$  thin films were prepared by electron beam evaporation on the glass substrates using high purity  $\text{Cu}_2\text{O}$  pellets. The vacuum chamber was pumped with the combination of diffusion pump and rotary pump and is capable of creating an ultimate vacuum of  $4 \times 10^{-4}$  Pa. The pressure was measured using combination of Pirani–Penning gauge. The pellet was prepared using high purity (99.99%)  $\text{Cu}_2\text{O}$  powder. The pellets were kept in a water-cooled copper crucible. The films were prepared with different thickness ranging from 133 to 257nm by adjusting the deposition time. The thickness of the films was monitored by quartz crystal thickness monitor. The deposition parameters maintained during the preparation of  $\text{Cu}_2\text{O}$  films are given in Table 1.

The chemical composition of the films was analyzed by Energy Dispersive Spectroscopy (EDS) attached with SEM of model Oxford instruments Inca Penta FET X3. The crystallographic structure of the films was analyzed by Seifert 3003TT X-ray diffractometer (XRD), using  $\text{Cu K}\alpha$  radiation ( $\lambda = 0.1546$  nm). The microstructure and surface morphology of the films was studied by scanning electron microscopy (SEM) and atomic force microscopy

(AFM), respectively. The electrical properties of the films were measured by using standard four-probe method. The optical transmittance of the films was recorded using a UV–Vis–NIR double beam spectrophotometry.

Table.1. Deposition Parameters Of Cu<sub>2</sub>O Films During Deposition

---

Deposition method	: electron beam evaporation
Power source	: e-beam power supply (3 kW)
Pellet	: Cu <sub>2</sub> O (10 mm dia and 3 mm thick)
Substrates	: Glass
Target to substrate distance	: 60 mm
Ultimate pressure (P <sub>U</sub> )	: 4x10 <sup>-4</sup> Pa
Evaporation pressure (P <sub>W</sub> )	: 3x10 <sup>-2</sup> Pa
Substrate temperature (T <sub>S</sub> )	: 473 K
Accelerating voltage	: 4 kV
Filament current	: 30 mA
Deposition time	: 5 to 21 min
Films thickness	: 133, 192 and 257 nm

---

### 3. RESULTS AND DISCUSSION

The stoichiometry of the films was influenced by the film thickness. Fig.1. shows the EDS spectra of Cu<sub>2</sub>O films at different film thickness. EDS results revealed that the films consists only oxygen and copper, and no reflections of impurity were detected. The films have excess oxygen at the film thickness of 133nm and it decreased with increasing the film thickness to 192nm. The films deposited at thickness of 192nm were nearly stoichiometric. Beyond this films thickness the stoichiometry of the films was deviated. The obtained composition results at different film thickness were listed in Table 2. The similar behavior was observed in dc magnetron sputtered NiO films by Reddy et al.[13]

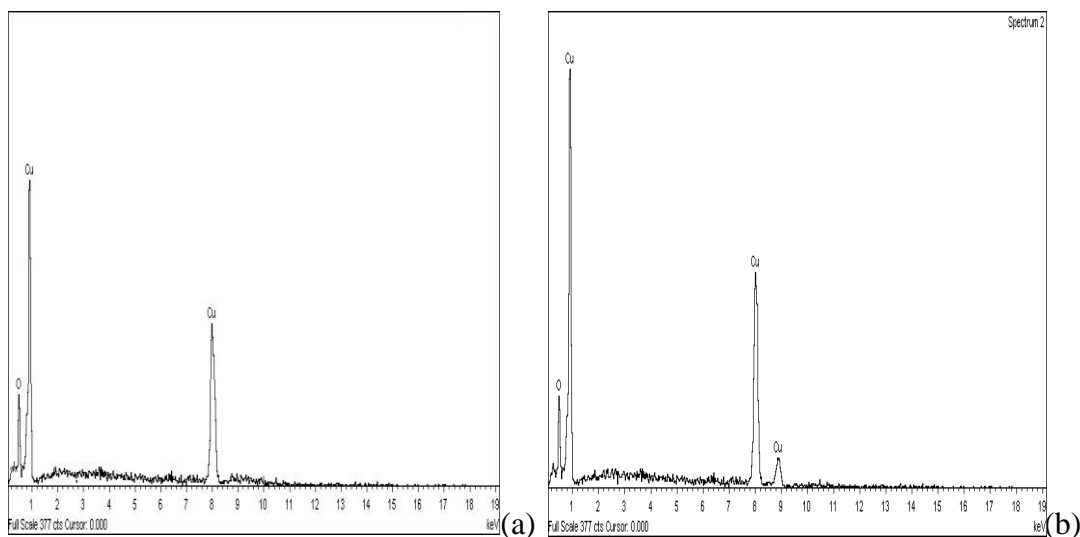


Fig.1. EDS spectra of  $\text{Cu}_2\text{O}$  films at different film thickness: (a) 133nm and (b) 192nm.

Table 2: The Compositional Results Of  $\text{Cu}_2\text{O}$  Films

Film thickness	Element	Atomic percentage
133nm	O K	41.56
	Cu K	58.44
192nm	O K	35.39
	Cu K	64.61

### 3.1. Structural Properties

Fig.2. shows the XRD spectra of  $\text{Cu}_2\text{O}$  films deposited at different film thickness. The thickness of the films was also influenced the structural properties. The films deposited at film thickness of 133nm shows a small peak with amorphous background. As increasing the films thickness to 192nm, the peak intensity and the polycrystalline nature increased. The peak intensity increases and become sharper when the films thickness increases, which is due to the better crystallinity of the films and grain size becomes larger. The large thickness (~192nm) may provide the sufficient space for thermal motion of particles, as a result the alignment of crystallites improve. The more thickness (<192nm) does not improve the crystallite size of the films. The broadening of the peak width at higher films thickness correlated to smaller grains in

the films. Balu et al. [14] observed the increasing of the crystallinity with thickness in electron beam evaporated ZnTe films. As increasing the film thickness from 133 to 192nm the peak position was shifted toward the lower angle side.

The average crystallite size of the Cu<sub>2</sub>O films at different thickness was calculated by using Scherrer's equation [15]. The obtained crystallite size at different film thickness is 10, 23 and 12nm for 133, 192 and 257nm, respectively. The increasing of the crystallite size with films thickness may be due to decrease of defects in lattice.

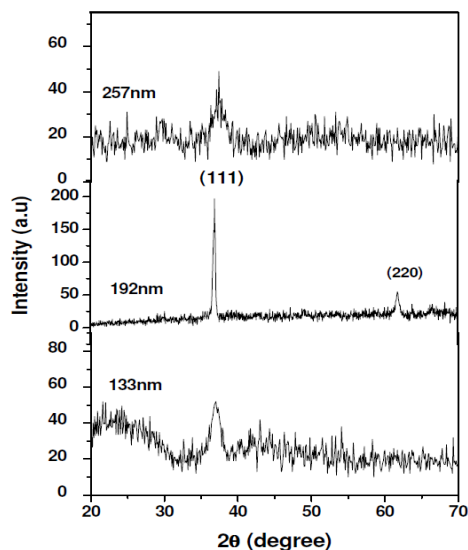


Fig.2. XRD patterns of Cu<sub>2</sub>O films at different film thickness

The lattice parameter (a) of the films was calculated using the following relation,

$$d = a / (h^2 + k^2 + l^2)^{1/2} \quad \text{-----(1)}$$

where h, k and l are the Miller indices. The interplaner spacing (d) was evaluated from the X-ray diffraction data using the Bragg's relation. The obtained lattice parameter values at different film thicknesses are lower than the standard value (ICDD = 4.269Å). The obtained lattice parameter values are 4.196, 4.226 and 4.164 Å for film thickness of 133, 192 and 257nm, respectively. The decreasing the lattice parameter with increasing the film thickness was due to stress developed in the films.

The change in the stress of films at different film thickness was analyzed. The stress ( $\sigma$ ) is calculated using the following relation [16]:

$$\sigma = -E(a-a_0)/2va_0 \text{ -----(2)}$$

where E is the Young's Modules of the Cu<sub>2</sub>O (30 GPa), 'a' is the lattice parameter of the bulk material, 'a<sub>0</sub>' the measured lattice parameter and 'v' the Poisson's ratio (0.455). The films exhibited compressive stress and it decreased with increasing of the thickness. The calculated stress values are -0.57, -0.34 and -0.83Gpa for 133, 192 and 257nm. The different types of stress developed in the films during the deposition is may be due to collision of ablation particles with the substrate at a high energy, thermal expansion between the substrate and film, and lattice mismatch between the substrate and film [17].

### 3.2. Microstructure and Surface Morphology

Fig.3. shows the SEM images of Cu<sub>2</sub>O films at different film thickness. The films deposited at thickness of 192nm exhibits quite uniform surface with larger grain size than the thinner films. As increasing the thickness, the films are more homogeneous with reduced structural defects, which lead the increasing of the grain size. At higher thickness films exhibited island and small grains.

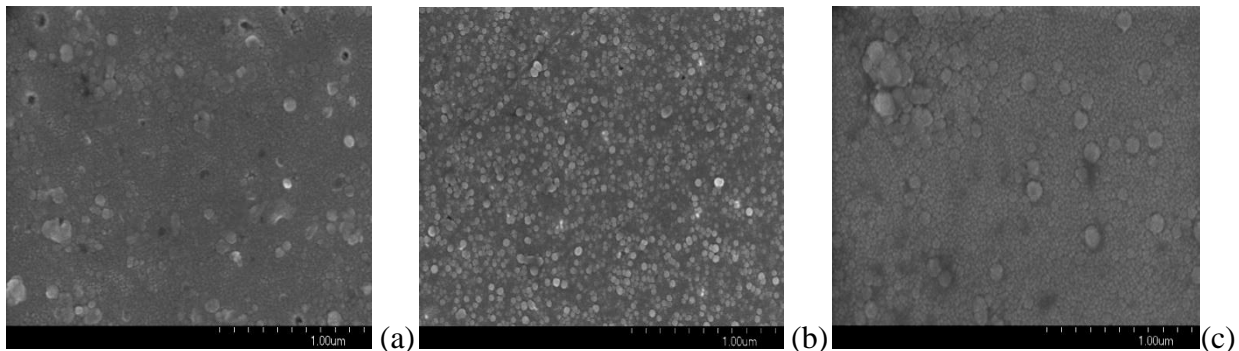


Fig.3. SEM images of Cu<sub>2</sub>O films at different film thickness: (a) 133, (b) 192 and (c) 257nm

The surface roughness is an important aspect since it influences the electrical and optical properties of the films. Fig.4. shows the surface morphologies of the films deposited at different film thickness. The films deposited at lower thickness there are many nucleation centers on the substrate and produced small grains. The small grains on the substrate are not able to grow into

large size, thus the lower thickness films have smaller grains. As increasing the films thickness, the crystallinity of the films is enhanced and the grains become larger [18]. The surface roughness of the films decreased with increasing the film thickness upto 192nm, and it increased at higher film thickness. The obtained surface roughness of the films is 4.7, 2.8 and 3.9nm for 133, 192 and 257nm, respectively. The high surface roughness of the films at thickness of 133 and 257nm was due to presence of islands and fine grains.

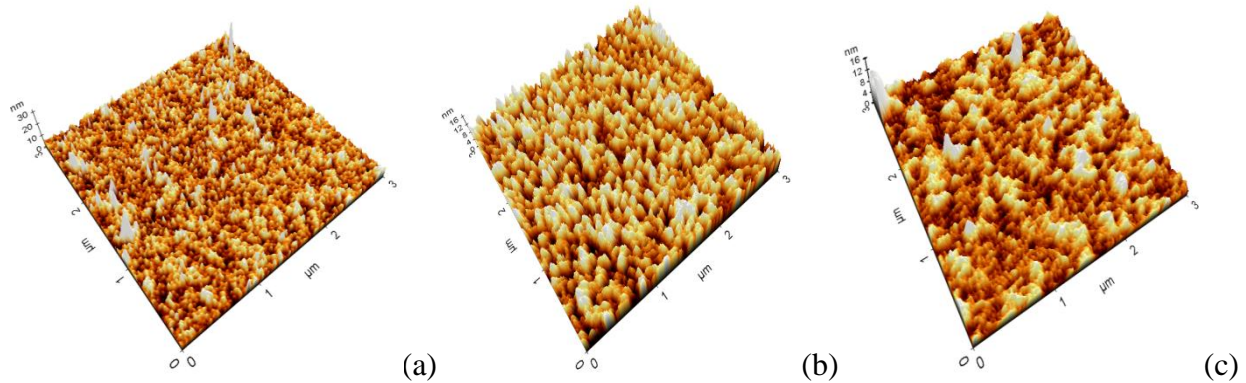


Fig.4. AFM images of Cu<sub>2</sub>O films at different film thickness: (a) 133, (b) 192 and (c) 257nm

### 3.3. Electrical and Optical Properties

The electrical properties of Cu<sub>2</sub>O films at different film thickness are listed in Table 3. The resistivity and carrier concentration of the films decreases with increasing the film thickness to 192nm, whereas the mobility of the films increases. The increasing of the mobility with films thickness was due to the improved crystallinity and grain size of the films.

It is known that the optical properties have strong correlation with the structural and surface morphology such as density of defects, crystallinity and surface roughness of the films. Fig.5. shows the optical transmittance spectra of Cu<sub>2</sub>O films at different film thickness. The poor optical transmittance was observed at low and very high thickness films. The films deposited at film thickness of 192nm shows high optical transmittance of 79%. The optical transmittance of the films increased from 32% to 60% with increasing the film thickness from 150 to 350nm in dc magnetron sputtered NiO thin films, which was due to high surface light scattering of the films and poor crystallinity of the films [13].

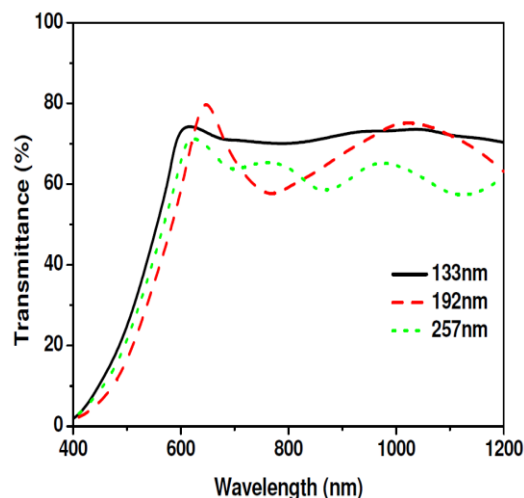


Fig.5. Optical transmittance spectra of Cu<sub>2</sub>O films at different film thickness

The refractive index ( $n$ ) of the films was calculated using the Swanepoel's envelope method [19] from the transmittance spectra. The obtained refractive index values are 2.29, 2.35, 2.31 for film thickness of 133, 192 and 257nm respectively. The similar changes of refractive index with films thickness was observed in rf magnetron sputtered ZnO films[20].

Fig.6. shows the  $(\alpha h\nu)^2$  versus photon energy of Cu<sub>2</sub>O films at different film thickness. The films show the high optical band gap at thickness of 133 and 257nm (Table 3). The band gap energy decreased from 2.47 to 2.3eV with increase in the deposition time from 300 to 600s was observed in electrodeposited Cu<sub>2</sub>O films [21]. Chander et al.[22] observed the decreasing of the band gap at higher thickness in electron beam evaporated CdZnTe film, which was due to increase of structural defect, mobility, disorder at the grain boundaries, stoichiometric deviation and quantum size effect change.

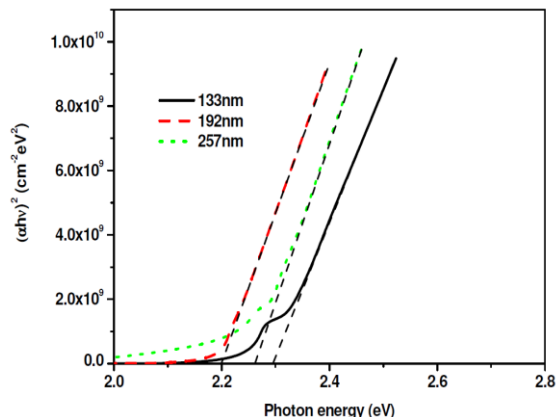


Fig.6.  $(\alpha h\nu)^2$  versus the photon energy  $(h\nu)$  of  $\text{Cu}_2\text{O}$  films at different film thickness

Table 3. Electrical And Optical Properties Of  $\text{Cu}_2\text{O}$  Films At Different Film Thickness

Thickness	Resistivity ( $\Omega\text{cm}$ )	Hall mobility ( $\text{cm}^2/\text{V}\cdot\text{sec}$ )	Carrier concentration ( $\text{cm}^{-3}$ )	Transmittance (%) at $\lambda=650\text{ nm}$	Band gap (eV)
133nm	77	2.5	$3.2 \times 10^{16}$	68	2.29
192nm	31	7.2	$2.8 \times 10^{16}$	79	2.20
257nm	44	3.7	$3.9 \times 10^{16}$	63	2.26

#### 4. CONCLUSIONS

$\text{Cu}_2\text{O}$  films of have been deposited on glass substrates by electron beam evaporation. From XRD results, the films deposited at film thickness of 192 exhibited better crystallinity and smooth surface. The obtained lattice parameter values are lower than the standard value. The structural and surface morphology of the films improved with film thickness. The films deposited at thickness of 192nm exhibited smooth surface with optical band gap of 2.20 eV and electrical resistivity of  $31\Omega\text{cm}$ .

## REFERENCES

- [1] Y. Hwang, H. Ahn, M. Kang, Y. Um, *Current Applied Physics* 15, S89-S94, 2015.
- [2] Z. Jin, X. Zhang, Y. Li, S. Li, G. Lu, *Catal. Commun.* 8, 1267-1273, 2007.
- [3] L. Fu, J. Gao, T. Zhang, Q. Cao, L.C. Yang, Y.P. Wu, R. Holze, *J. Power Sources* 171, 904-907, 2007.
- [4] H.A. Al-Jawhari, *Mater. Sci. Semicond. Process.* 40, 241-252, 2015.
- [5] X. Jiang, Q. Lin, M. Zhang, G. He, Z. Sun, *Nanoscale Research Letters* 10:30, 2015.
- [6] K. Lim, J.Park, D-G. Kim, J-K. Kim, J-W. Kanga, Y-C. Kang, *Appl. Surf. Science* 258, 9054-9057, 2012.
- [7] S. Dolai, S. Das, S. Hussain, R. Bhar, A.K. Pal, *Vacuum* 141, 296-306, 2017.
- [8] M-Y. Lin, C-Y. Lee, S-C. Shiu, I-J. Wang, J-Y. Sun, W-H. Wu, Y-H. Lin, J-S. Huang, C-F. Lin, *Organic Electronics* 11, 1828-1834, 2010.
- [9] A. Ashida, S. Sato, T. Yoshimura, N. Fujimura, *J. Crystal Growth* 468, 245-248, 2017.
- [10] A. Karapetyan, A. Reymers, S. Giorgio, C. Fauquet, L. Sajti, S. Nitsche, M. Nersesyan, V. Gevorgyan, W. Marine, *J. Luminescence* 159, 325-332, 2015.
- [11] H. Sun, S-C. Chen, C-K. Wen, T-H. Chuang, M.A.P. Yazdi, F. Sanchette, A. Billard, *Ceramic International* 43, 6214-6220, 2017.
- [12] R. Oommen, U. Rajalakshmi, Sanjeeviraja, *Int. J. Electrochem. Sci.*, 7, 8288-8298, 2012.
- [13] A. Mallikarjuna Reddy, A. Sivasankar Reddy, P. Sreedhara Reddy, *Vacuum* 85, 949-954, 2011.
- [14] A.R. Balu, V.S. Nagarethinam, A. Thayumanavan, K.R. Murali, C. Sanjeeviraja, M. Jayachandran, *J. Alloys and Compounds* 502, 434-438, 2010.
- [15] B.D. Cullity, *Elements of X-ray Diffraction*, second ed., Addison Wesley, London
- [16] M. Ohring, *The Material Science of Thin Solid Films*, Academic Press, New York, 1992.
- [17] H.W. Song, K. No, *J. Korean Physical Society*, 58, 809-816, 2011.
- [18] X. Yu, J. Ma, F. Ji, Y. Wang, C. Cheng, H. Ma, *Applied Surface Science* 245, 310-315, 2005.
- [19] R. Swanepoel, *J. Phys. E. Sci. Instrum.* 16, 1214, 1983.
- [20] R. Subba Reddy, A. Sreedhar, A. Sivasankar Reddy, S. Uthanna, *Adv. Mat. Lett.*, 3, 239-245, 2012.
- [21] O. Messaoudi, I. Ben assaker, M. Gannouni, A. Souissi, H. Makhlof, A. Bardaoui, R.

Chtourou, Applied Surface Science 366, 383-388, 2016.

[22] S. Chander, M.S.Dhak, Physica E 84, 112-117, 2016.